www.ksmrm.org JKSMRM 16(3) : 205-216, 2012
Print ISSN 1226-9751

Original Article

# Invasive Micropapillary Carcinoma of the Breast: Mammographic, Sonographic and MR Imaging Findings

**Sun Jung Rhee, Boo-Kyung Han, Eun Young Ko, Jung Hee Shin**

Department of Radiology and Center for Imaging Science, Samsung Medical Center, Sungkyunkwan University School of Medicine, Seoul, Korea

**Purpose :** We performed this study to investigate the characteristic imaging and clinicopathologic features of invasive micropapillary carcinoma of the breast.

**Materials and Methods:** Among the 47 women with surgically confirmed invasive micropapillary carcinoma between 2005 and 2009, 32 patients (mean age, 50 years; range, 37–69 years) had all preoperative mammography, ultrasound (US) and MR images. Two radiologists retrospectively assessed the imaging findings, clinical presentation and histological results of the patients.

**Results:** On mammography, 29 of 32 patients had suspicious findings. Among them, a mass (or focal asymmetry) with calcifications was the most common findings (15/32, 65%). The calcifications were noted in 20 patients (63%) and the shape of calcifications was frequently amorphous or punctate (n = 12, 60%). On US and MR imaging, all lesions had suspicious findings. The most common US findings were single (n = 20) or multiple (n = 10) irregular hypoechoic mass (es). The mass was frequently hypoechoic (n = 29, 97%). On MR imaging, the type of lesions was a mass or masses in 23 (72%), a mass combined with non-mass in six patients, and non-mass lesions in three patients. Histologically, axillary lymph nodes metastasis were very common (25/32, 78%). Asymptomatic clinical presentation was not usual (9/32, 28%).

**Conclusion:** The imaging features of invasive micropapillary carcinomas strongly suggest malignancy. Microcalcifications on mammography, marked hypoechogenicity on US and an irregular mass, often combined with non-mass on MR are common. Axillary lymph node metastasis is commonly associated.

**Index words :** Breast · Carcinoma · Invasive micropapillary carcinoma · MR imaging · Sonography

## INTRODUCTION

Invasive micropapillary carcinoma (IMPC) of the breast is a rare variant of invasive ductal carcinoma, which accounts for 0.7–3% of all breast cancers (1, 2). IMPC is a unique pathologic entity characterized by pseudo-papillary structures floating in empty, clear spaces lined by delicate strands of stroma. IMPC shows clinically aggressive prognosis with invasion to lymphatic system, extensive axillary lymph node involvement, frequent local recurrence and distant metastasis. This tumor has been described as a morphologically distinctive entity by Petersen in 1993 (2) and several articles on IMPC are found in the pathology literature (1, 3–6), but a few articles has described its imaging features (7, 8). Knowledge of the imaging findings of IMPC would be useful to diagnose this disease. IMPC is rare variant of the breast cancer, but clinician and radiologist can regard this disease as

• Received; June 25, 2012 • Revised; November 26, 2012
• Accepted; December 27, 2012
Corresponding author : Boo-Kyung Han, M.D.
Department of Radiology and Center for Imaging Science, Samsung Medical Center, Sungkyunkwan University School of Medicine, 50, Irwon-dong, Gangnam-gu, Seoul 135-710, Korea.
Tel. 82-2-3410-0517, Fax. 82-2-3410-0084
E-mail : bkhan@skku.edu

one of the possible diagnosis. However, there is scant information in the medical literature describing this topic.

The purpose of this study is to retrospectively evaluate the imaging findings of IMPC and to identify the characteristic imaging and clinical findings.

## MATERIALS AND METHODS

### Patient selection

In our breast surgery database, from 2005 to 2009, 4,139 women underwent breast cancer surgeries. Among them, 47 had been diagnosed with IMPC of the breast and 32 of them had undergone all three preoperative images of mammography, ultrasonography (US), and magnetic resonance (MR) imaging. We excluded 15 patients who didn't perform the preoperative MR imaging. The mean age was 50 years; range, 37–69 years at the time of diagnosis. The mode of presentation was divided into symptomatic or asymptomatic presentation. This study was approved by our institutional review board. As images were analyzed retrospectively, the requirement for informed consent was waived.

### Image review

Two radiologists who are specialized in breast imaging retrospectively reviewed all the preoperative images in consensus. All the imaging findings were described using the American College of Radiology (ACR) Breast Imaging Reporting and Data System (BI-RADS) lexicon (9) with some modification.

Standard two-view mammography was performed with digital mammography equipment (Senographe 2000D or DMR; General Electric Medical Systems, Buc, France). Breast parenchymal density was categorized as fatty, heterogeneously dense, and extremely dense according to the lexicon (9). Mammograms were reviewed for type of lesions (mass or asymmetry with calcifications, mass or asymmetry without calcifications, calcifications only and negative findings), shape of microcalcifications.

US examinations were performed with 7–12 MHz linear transducer (HDI 3000, 5000 or iU22; Philips Medical Systems, Bothell, WA or Logiq 700; General Electric, Milwaukee, WI) by radiologists. Sonograms were assessed for the type of the lesion (mass, non-mass-forming heterogeneity), shape, margin, and echogenecity. According to BI-RADS lexicon, the echogenecity of mass is classified as hyperechoic, isoechoic, hypo echoic and anechoic. Because hypoechogenicity has a wide range, we divided hypoechogenicity into "mildly hypoechoic," which was slightly less echogenic than subcutaneous fat tissue and "markedly hypoechoic," which was much more hypoechoic approaching to blackness. We analyzed the category of the lesions according to the radiologic reports.

MR imaging was performed at 1.5 T with a whole-body imaging system (Signa EXCITE; GE Healthcare, Milwaukee, Wis, Achieva; Philips) and a dedicated four-channel breast coil. The patient was prone, and images were acquired with the following sequences: unenhanced axial T1-weighted spin echo (TR/TE, 500/10); axial T2-weighted fat-suppressed fast spin echo (5500/70); dynamic contrast enhanced axial or

**Table 1. Imaging and Clinicopathologic Findings of 32 patients with Invasive Micropapillary Carcinoma**

| Imaging and Clinicopathologic Findings | Number (%) |
|---|---|
| Mammography | |
| Mass (or asymmetry) with calcifications | 15 (47) |
| Mass (or asymmetry) without calcifications | 9 (28) |
| Calcifications only | 5 (16) |
| Shape of calcifications | 20 (63) |
| punctate or amorphous | 12 (60) |
| fine pleomorphic or coarse heterogeneous | 8 (40) |
| Negative | 3 (9) |
| Ultrasonography | |
| Mass (or masses) | 30 (94) |
| Single mass | 20 (67) |
| Multiple masses | 10 (33) |
| Non-mass forming heterogeneity | 2 (6) |
| MR imaging | |
| Mass | 23 (72) |
| Non-mass lesion | 9 (28) |
| Clinical presentation | |
| Symptomatic | 23 (72) |
| Palpable mass | 22 (69) |
| Bloody nipple discharge | 1 (3) |
| Asymptomatic | 9 (28) |
| Mammography-detected | 6 (19) |
| Ultrasonography-detected | 2 (6) |
| Positron emission tomography-detected | 1 (3) |
| Histological lymph node metastasis | 25 (78) |
| US or MR imaging positive | 16 (50) |
| Neither imaging positive | 9 (28) |

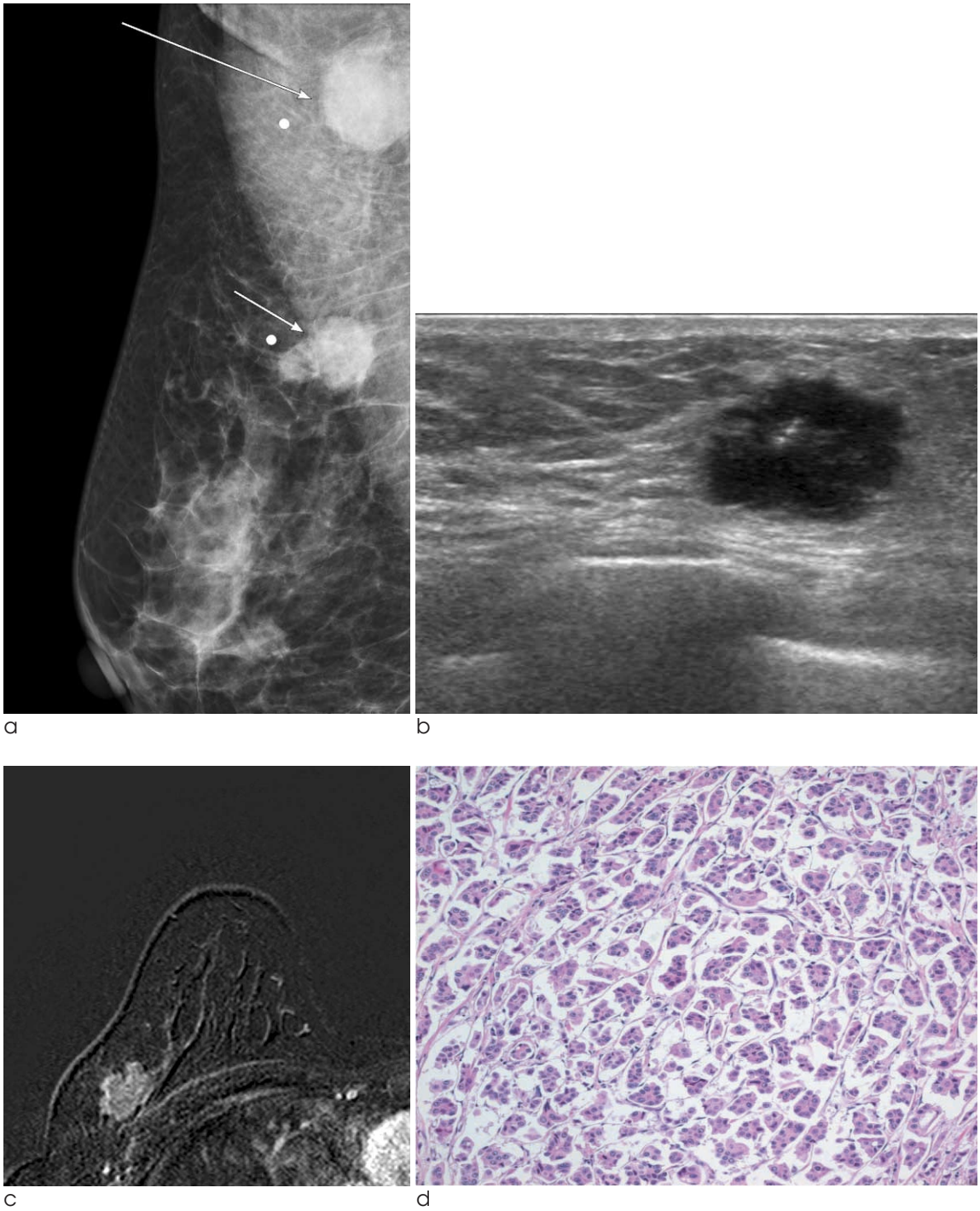


**Fig. 1.** 54-year-old woman with a palpable mass.

**a.** A mediolateral oblique mammogram shows a 2.3-cm ill-defined hyperdense mass with multiple amorphous or punctate microcalcifications (short arrow). Right axillary lymph node was also enlarged (long arrow).

**b.** A sonogram shows an irregular markedly hypoechoic mass. An enlarged lymph node was also seen (not shown here).

**c.** A subtraction MR image of spoiled gradient echo sequence (SPGR) 1 minute after contrast injection shows a 2.2-cm, intensely enhancing, irregular mass with rim enhancement. The histologic result was a 2.2 cm, IMPC grade III with metastasis to one axillary lymph node.

**d.** Photomicroscopic examination reveals invasive carcinoma characterized by compact tumor cell clusters within prominent clear spaces, which resemble dilated lymphatic vessels (Hematoxylin and eosin stain, ×200). These clear spaces are known to be actually artifacts made by formalin fixation or paraffin embedding, not real spaces. Marked hypoechogenicity on US might be related with uniform hypercellularity.

sagittal T1-weighted 3D fat-suppressed fast spoiled gradient echo (18/4; flip angle, 15°) sequences, which was dynamically obtained 3 to 6 times after the use of gadopentate dimeglumine (0.1 mmol per kilogram body weight; Gadovist, Schering, Berlin, Germany). The field of view was 160–220 mm, and the matrix size was 256 × 256 pixels. After examination, two subtraction images were automatically made on a pixel-by-pixel basis: the un-enhanced images were subtracted from the early post-contrast images (standard subtraction), and the last post-contrast images were subtracted from the early post-contrast images (reverse subtraction). The reformatted images with a maximum intensity projection were then created from the standard and reverse subtraction images. Areas of abnormal enhancement were

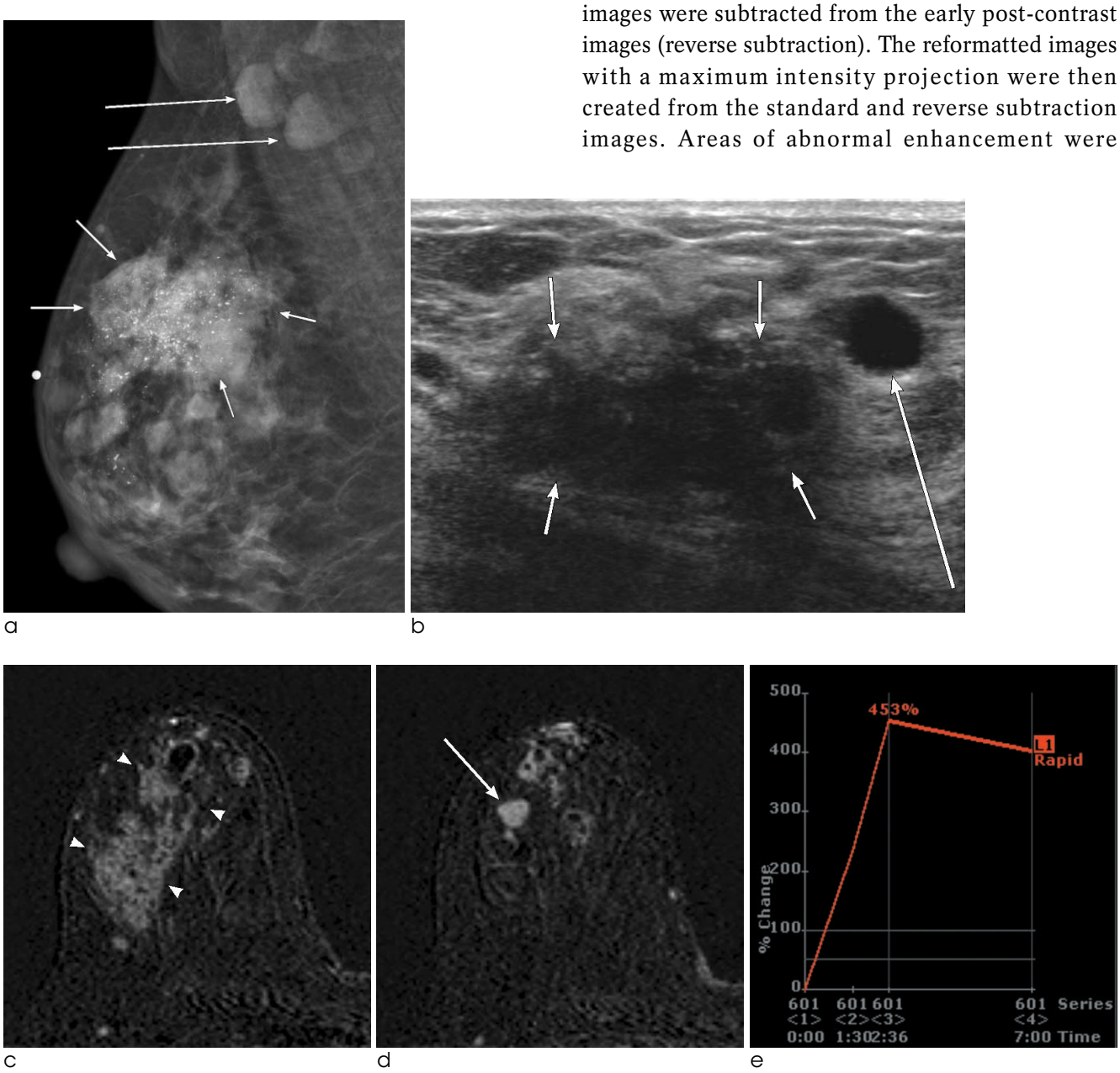


**Fig. 2.** Fig. 2. 56-year-old woman with a palpable mass.

**a.** A mediolateral oblique mammogram shows global asymmetry with multiple coarse heterogeneous microcalcifications (short arrows) and enlarged axillary lymph nodes (long arrows).

**b.** A sonogram shows a large irregular markedly hypoechoic mass (short arrows) and a satellite hypoechoic mass (long arrow).

**c, d.** Subtraction MR imaging of SPGR 1 minute after contrast injection show a non-mass lesion (arrowheads) with clumped segmental pattern and an intensely enhancing mass (arrow). Neoadjuvant chemotherapy was conducted and a final pathology showed two IMPCs with widespread DCIS in a 7-cm segment. Axillary lymph node metastasis was histologically not associated after neoadjuvant chemotherapy.

**e.** The kinetic curve obtained from the most enhanced area shows early rapid enhancement and washout pattern.

described as mass or non-mass like, and enhancement kinetics, especially focused on the washout pattern, were reviewed. The kinetic curves were analyzed by using a computer aided detection (CAD) software (CADstream).

### Histopathologic review

Histopathologic diagnosis was made by the surgical excision. We reviewed pathologic report for assessment of the tumor size, nuclear grade, histologic grade, presence of endolymphatic tumor emboli and axillary lymph node. We reviewed the pathologic result of immunohistochemical analyses for estrogen receptor (ER), progesterone receptor (PR), and c-erb B-2.

## RESULTS

### Patients

The imaging findings, clinical presentation, and pathologic findings are summarized in Table 1. Clinical symptom was associated with 23 of 32 patients (72%). IMPCs were diagnosed from palpable breast masses in 22 patients (69%) and bloody nipple discharge in one (3%). Nine patients (28%) had an incidental abnormality detected on screening mammography (n = 6), US (n = 2) or positron emission tomography (n = 1). The right breast was involved in 18 patients (56%) and the left breast in 14 patients (44%).

### Mammography

The background parenchymal density was BI-RADS type 1 pattern in 1, type 2 pattern in 8, type 3 in 16, type 4 in 7 patients. The mammographic findings in 32 patients were as follows: mass or focal asymmetry with calcifications in 15 (47%) (Figs. 1–3), calcifications only in 5 (16%) (Fig. 4), mass or asymmetry in 9 (28%) (Fig. 5), and no abnormality in 3 (9%) patients (Fig. 6). Microcalcifications were present in 20 (63%) patients; amorphous or punctate calcifications (Figs. 1, 3) in 12 (60%) and coarse heterogeneous calcifications

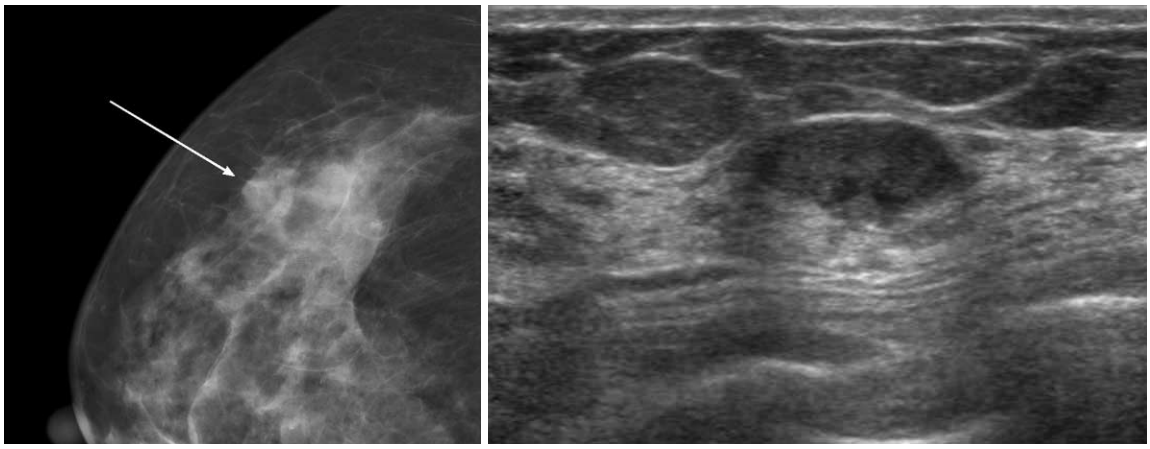

a b

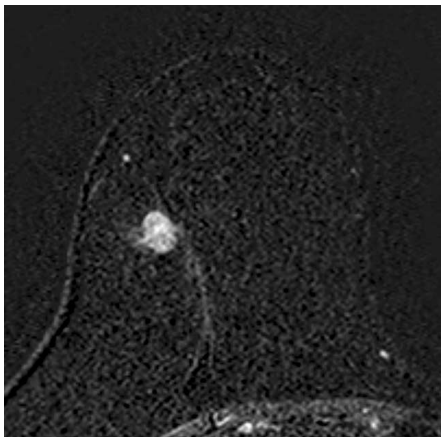

c

**Fig. 3.** 64-year-old woman with an abnormal uptake on positron emission tomography.
**a.** A craniocaudal mammogram shows a focal asymmetry with punctate microcalcifications (arrow) in right outer breast.
**b.** A sonography shows a circumscribed oval, isoechoic mass at the same area.
**c.** A subtraction MR image shows an ovoid mass with rapid enhancement. The histologic result was a 1.5 cm, IMPC grade III without endolymphatic tumor emboli.

(Fig. 2) or fine pleomorphic (Fig. 4) in 8 (40%). All the positive mammographic findings were typical of malignancy and classified into BI-RADS category 5 (definitive malignancy).

### Ultrasonography

Sonographic findings of 32 patients are presented in Table 2. On US, the abnormal findings were seen in all cases and classified into BI-RADS category 4b (n = 8), 4c (n = 6), or 5 (n = 18). A single mass (n = 20) or multiple masses (n = 10) were visible in 30 (94%) patients (Figs. 1–3, 5–6), and non-mass like heterogeneity was found in two patients (6%) (Fig. 4). The mean tumor size on ultrasonography was 2.3 cm (range, 0.8–8.0 cm). The masses usually showed an irregular shape and hypoechogenicity in all except one (Figs. 1, 2, 5, 6). The echogenicity was especially markedly hypoechoic in 20 (20/30, 66.7%) (Figs. 1, 2, 5). Most of the masses showed suspicious findings in their margin: indistinct (n = 6), microlobulated (n = 8) and spiculated (n = 15). Only one mass detected during work-up of abnormal uptake of positron-emission tomography-computed tomography (PET-CT) showed an oval circumscribed isoechoic mass (Fig. 3). The sonographic finding of the mass seemed to

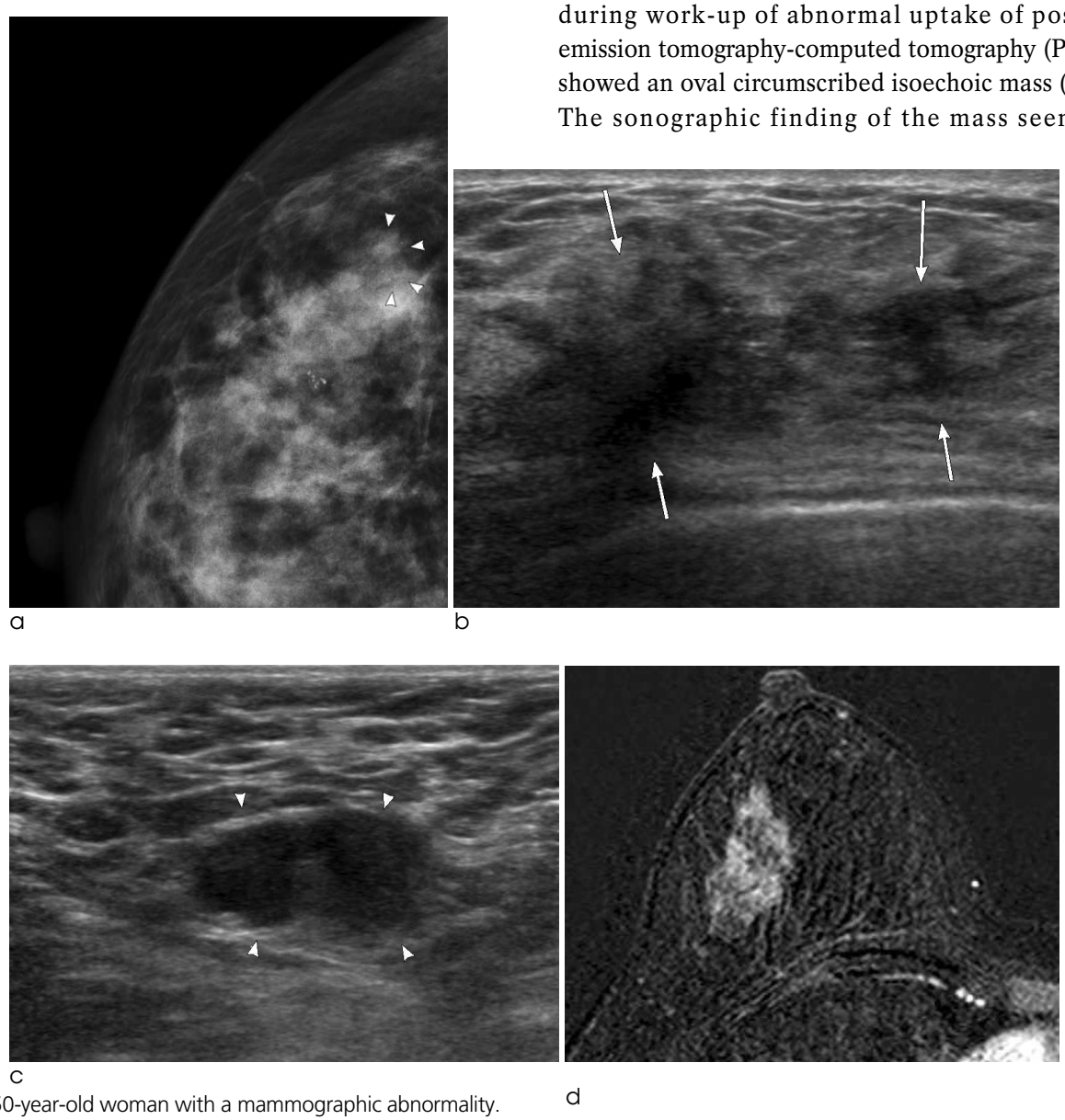


**Fig. 4.** 50-year-old woman with a mammographic abnormality.
**a.** A craniocaudal mammography shows clustered fine pleomorphic calcifications (arrowheads).
**b, c.** Sonograms show an ill-defined non-mass like heterogeneity with shadowing (**b**, arrows) and an enlarged lymph node in the right axilla (arrowheads) (**c**).
**d.** A subtraction MR image of SPGR 1 minute after contrast injection shows non-mass enhancement (arrows) with clumped segmental pattern. The histologic result was 4.6-cm, IMPC grade III with axillary lymph node metastasis (6 of 28 dissected lymph nodes).

probably benign mass, but it shows increased uptake on PET-CT and it categorized to BI-RADS category 4b. The two cases, a suspicious mass was detected during supplemental US screening and the mass showed typical malignant features (Fig. 6).

### MR imaging

On MR imaging, the abnormal findings were seen in all cases and classified into BI-RADS category 4c or 5. The type of lesions was a single mass or multiple masses in 23 (72%) (Figs. 1, 3, 5, 6), mass associated with non-mass like enhancement in 6 (19%) (Fig. 2), and only non-mass like enhancement in 3 (9%) (Fig. 4). Of the 23 mass lesions, the shape of the mass was irregular in 19 and oval or lobular in 4. The margin was irregular or spiculated in 16 (Figs. 1, 5) and smooth with rim enhancement in seven (Figs. 3, 6). Of the 9 non-mass like enhancing lesions, seven showed clumped segmental pattern (Fig. 4), and two showed regional heterogeneous pattern.

On dynamic MR kinetics, all lesions showed initial rapid enhancement and 29 (91%) lesions showed washout kinetics (Figs. 2, 5) and three (9%) lesions showed persistent enhancement. In two lesions, trabecular thickening and enhancement were noted like inflammatory breast cancers.

Multiplicity was observed in ten (31%) cases. In one case, MR imaging depicted a tumor in the contralateral breast that was mammographically and sonographically occult. MR imaging also detected another malignant lesions in the ipsilateral breast that were mammographically and sonographically occult in three cases.

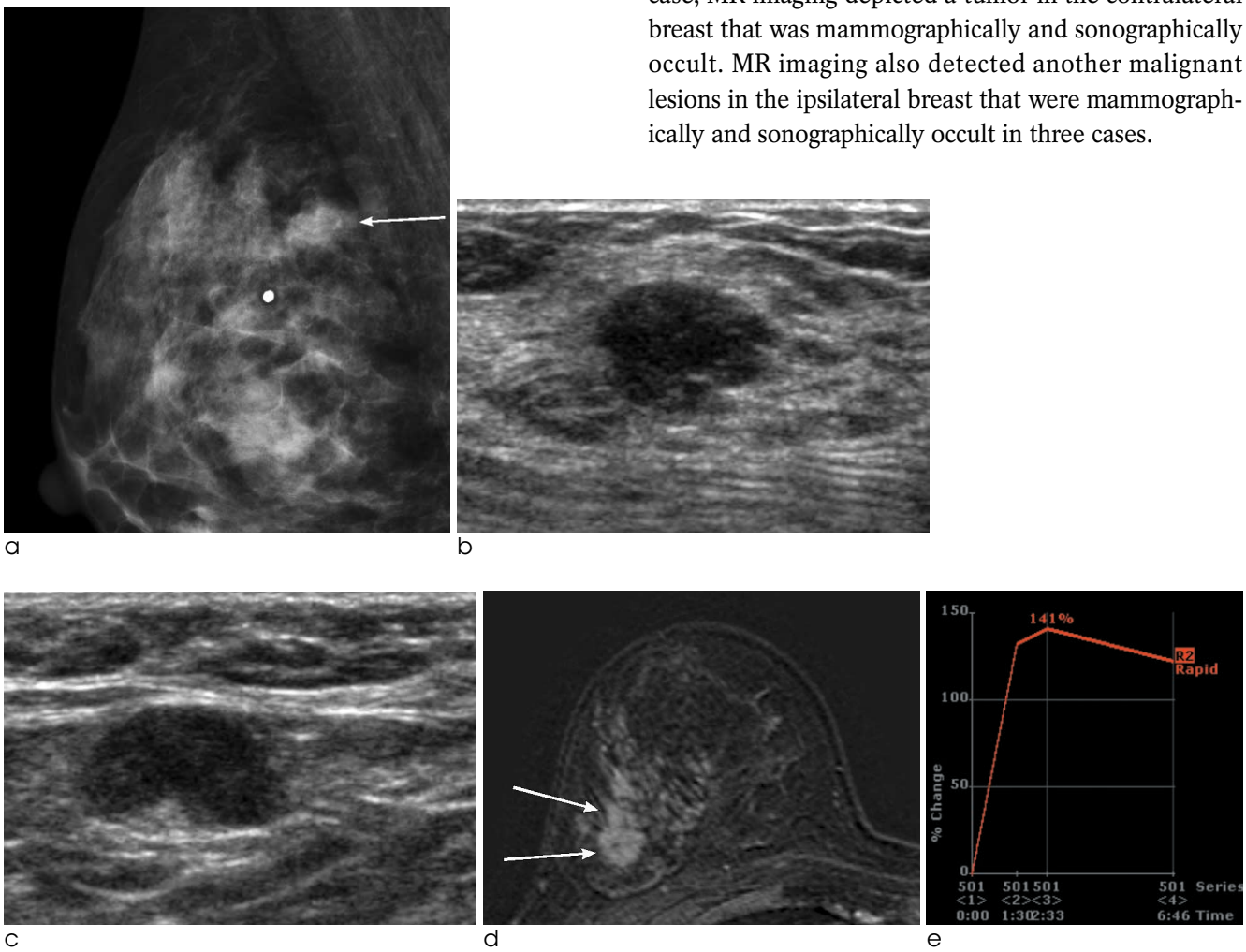


**Fig. 5.** 46-year-old woman with a palpable mass.
**a.** A mediolateral oblique mammogram shows a 1-cm ill-defined hyperdense mass (arrow).
**b, c.** Sonograms show a 1-cm, irregular markedly hypoechoic mass (**b**) with an enlarged lymph node (**c**).
**d.** A subtraction MR image shows a 2-cm, intensely enhancing, irregular mass, a little larger than US and mammography (arrows). The histologic result was a 2 cm, IMPC grade III with metastasis to two axillary lymph nodes. There were no extensive intraductal components within the tumor.
**e.** The kinetic curve obtained from the most enhanced area shows early rapid enhancement and washout pattern.

### Histopathologic findings

Sixteen patients (50%) underwent modified radical or total mastectomy due to the large size of invasive tumors or wide area of ductal carcinoma in situ (n = 14), subareolar location (n = 1) and the patient's request (n = 1). Nine patients underwent neoadjuvant chemotherapy before the surgery. The mean tumor size in the patients who did not receive neoadjuvant chemotherapy (n = 23) was 1.9 cm (range, 1.0–4.6 cm) and among them, 16 had T1 cancers (tumor size < 2 cm). Nuclear grade was high in 22 (67%), intermediate in eight (25%), and low in 2 (6%). Histologic grade was poorly-differentiated in 14 cases (44%), moderately differentiated in 16 (50%), and well-differentiated in 2 (6%). Endolymphatic tumor emboli were seen in 27 (84%) cases. Histologic axillary lymph node metastasis was present in 25 (78%) cases (Figs. 1–4). Among the cases with lymph node metastasis, the suspicious lymph nodes were seen in 16 cases (64%) on preoperative US or MR images. In 6 of them, the enlarged lymph nodes were seen as only equivocal cortical thickening less than 3 mm on US but US-guided aspiration revealed a metastasis in all cases.

Immunohistochemical analyses were available for all patients. The analysis showed the expression of ERs in 81.2% of the cases (26 of 32), PRs in 71.8% of the cases (23 of 32) and c-erbB-2 in 42.7% of the cases (14 of 32).

**Table 2. Ultrasonographic Findings of 32 patients with Invasive Micropapillary Carcinoma**

| Ultrasonographic Findings | Number (%) |
|---|---|
| Mass | 30 (94) |
| Shape | |
| Oval | 1 (3) |
| Round | 0 (0) |
| Irregular | 29 (97) |
| Orientation | |
| Parallel | 17 (57) |
| Nonparallel | 13 (43) |
| Margin | |
| Circumscribed | 1 (3) |
| Indistinct | 6 (20) |
| Angular | 0 (0) |
| Microlobulated | 8 (27) |
| Spiculated | 15 (50) |
| Echotexture | |
| Anechoic | 0 (0) |
| Hyperechoic | 0 (0) |
| Complex | 0 (0) |
| Hypoechoic | 29 (97) |
| Isoechoic | 1 (3) |
| Non-mass forming heterogeneity | 2 (6) |
| Category | |
| 4b | 8 (25) |
| 4c | 6 (19) |
| 5 | 18 (56) |

## DISCUSSION

To our knowledge, our study of 32 patients with IMPC is the largest series to date describing the MR

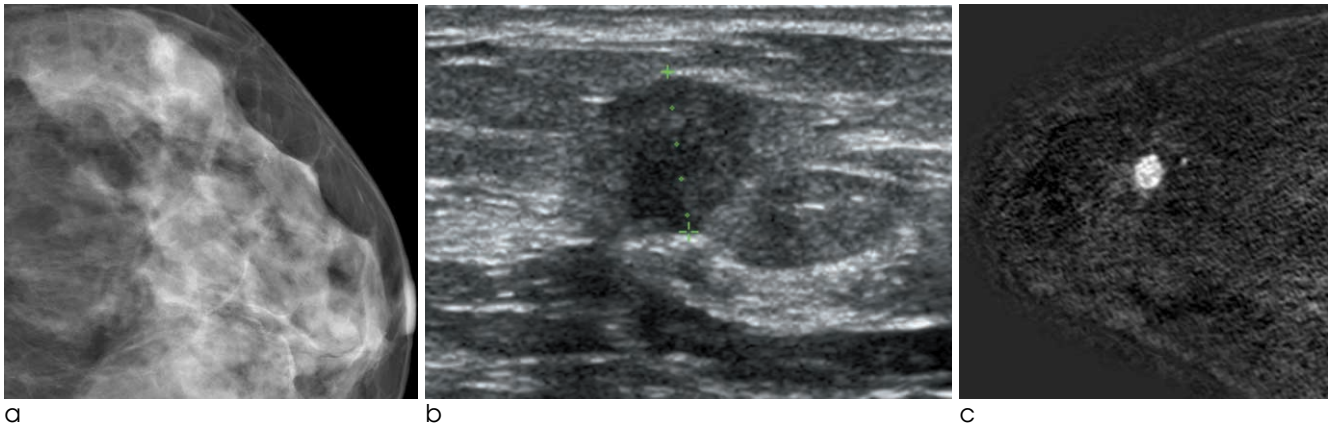

a b c

**Fig. 6.** 45-year-old woman with a sonographic abnormality.
**a.** A craniocaudal mammogram shows no abnormality.
**b.** A supplmental screening sonography shows an irregular hypoechoic mass in the left outer breast.
**c.** A subtraction MR image shows an ovoid mass with rim enhancement. The histologic result was a 1.4 cm, IMPC grade II with endolymphatic tumor emboli and EIC component.

**Table 3. MR Findings of 32 patients with Invasive Micropapillary Carcinoma**

| MR Findings | Number (%) |
|---|---|
| Mass | 23 (72) |
| Shape | |
| Oval | 3 (13) |
| Round | 1 (4) |
| Lobular | 0 (0) |
| Irregular | 19 (83) |
| Margin | |
| Smooth | 7 (30) |
| Irregular | 11 (48) |
| Spiculated | 5 (21) |
| Mass enhancement | |
| Homogenous | 2 (9) |
| Heterogous | 16 (70) |
| Rim enhancement | 5 (21) |
| Dark internal septation | 0 (0) |
| Enhancing intenal septation | 0 (0) |
| Central enhancement | 0 (0) |
| Nonmass Enhancement | 9 (28) |
| Distribution | |
| Focal area | 0 (0) |
| Linear | 0 (0) |
| Ductal | 0 (0) |
| Segmental | 7 (78) |
| Regional | 2 (22) |
| Multiple regions | 0 (0) |
| Diffuse | 0 (0) |
| Internal Enhancement | |
| Homogenous | 0 (0) |
| Heterogenous | 2 (22) |
| Stippled, puntate | 0 (0) |
| Clumped | 7 (78) |
| Reticular, dendrite | 0 (0) |
| Kinetic Curve assessment | 32 |
| Slow/medium/rapid | 0/0/32 (0/0/100) |
| Persistent/plateau/washout | 3/0/29 (9/0/91) |
| Category | 32 |
| 4c | 4 (12) |
| 5 | 28 (88) |

imaging features of IMPCs of the breast. IMPC was first described as a morphologically distinctive entity by Petersen in 1993 (2). This rare variant of invasive ductal carcinoma shows advanced stage at diagnosis and the high rate of local recurrence and distant metastases. Histologically, this tumor is characterized by pseudopapillary structures lacking a fibrovascular core and tubuloalveolar arrangement of tumor cell clusters floating freely in clear empty spaces. For purposes of diagnosis, treatment, and prognosis, the identification of IMPC as a distinct variant of breast cancer is needed.

Clinically, IMPC is often confused with invasive papillary carcinoma or micropapillary DCIS. Invasive papillary carcinoma has frond-forming growth pattern supported by a fibrovascular core (10). It occurs as only a small focus of stromal invasion at the periphery of the lesion and may have various growth patterns, either retaining a papillary pattern or, more commonly, spreading as a ductal carcinoma of the usual type (10). On mammography, invasive papillary carcinoma is seen as a solitary round, oval, or lobulated circumscribed mass or as clusters of well-defined masses. Masses may be associated with microcalcifications. On sonography, single or multiple circumscribed solid of complex mixed cystic and solid masses. Invasive papillary carcinoma could not be differentiated from benign papillomas using these imaging features alone (10, 11). This has a slow growth rate and less axillary nodal involvement, so patients with invasive papillary carcinoma have a better prognosis than do other forms of ductal carcinomas. Contrast to this, micropapillary DCIS, a variant of DCIS, shows frond-forming growth pattern, but does not have a fibrovascular core. It often ramify extensively in the ductal system (11). Since calcifications are usually not present and may be seen as architectural distortion on mammography, the modality of choice to determine the extent of the lesion is breast MR imaging (11, 12).

Clinically, the most common clinical manifestation of IMPC in our study was a palpable mass (69%), similar to previous studies (7, 8). There were 9 asymptomatic cases that were detected by screening examinations, mostly initially detected by mammography. The mammographic appearance of IMPC has been described in previous series as irregular shaped indistinct or spiculated high density mass with spiculated margin(13). Microcalcifications, either isolated or associated with a mass, were present in 43-68% in previous studies (7, 8, 13) and our group showed a similar rate (63%). Furthermore, in our series, the calcifications had more frequently amorphous or punctuate shape (60%).

Although there were 3 cases of mammographically negative IMPC, all lesions were seen on US and MR imaging both. The most common sonographic feature in our study was irregularly shaped solid mass without cystic change. The mass (es) was usually markedly,

homogeneously, hypoechoic. The marked homogeneous hypoechogenicity may represent high cellularity on histologic examinations. IMPC is usually composed of high nuclear grade malignant cells surrounded by clear spaces resembling lymphovascular channels and this hypercellularity may be related with homogeneous hypoechogenicity on US. On histopathologic comparison, the homogeneously hypoechoic pattern of the IPMC usually corresponded to the large-field, uniform cluster of tumor cells. In that pattern, acoustic impedances of the tumor were similar and differences in acoustic impedance were rare; therefore, the reflected echoes were less than those usually surrounding tissue, resulting in homogeneous hypoechogenicity (14). Posterior acoustic shadowing was not distinctive findings of this tumor like the other report (7, 8).

MR imaging is generally accepted as a more sensitive technique than mammography or sonography for the detection of breast cancers. The use of dynamic imaging and pharmacokinetics analysis of dynamic data has increased detection specificity (15, 16). In our study, a combined pattern with a mass and non-mass was observed in 6 cases (21%) on MR imaging. These were seen as a single mass on sonography. Intense heterogeneous enhancement, with rapid initial increase and washout kinetics on dynamic contrast-enhanced images was predominant (92%) and these features are characteristics of malignancy. MR imaging depicted additional malignancies which were mammographically and sonographically occult n the ipsilateral and contralateral breast. MR imaging was useful in assessing disease extent and multifocality before surgery.

Lymphatic vessel invasion and lymph node spread is frequent in IMPC and its incidence is reported to be 72–95% (17, 18). In our study, metastatic axillary lymph nodes were histologically confirmed in 25 breasts (78%). This prevalence is comparable to previous studies, which described metastatic lymph nodes in 80% of patients. This high positive rate of metastatic lymph nodes means that sentinel lymph node biopsy may not beneficial for these patients (12). Axillary lymph node metastasis was predicted well on ultrasound (64%), but even with equivocal cortical thickening less than 3 mm, lymph node metastasis was proved by US-guided fine needle aspiration. Due to high prevalence of lymphatic metastasis, normal-looking lymph nodes on US were frequently proved to have metastases.

Extensive intraductal component was observed in nine tumors (37%). Most of the tumors showed high nuclear grade (58%) and poorly differentiated histologic grade (50%). These are independent of aggressive behavior of IMPC (17).

IMPC is characterized by higher rates of ER and PR expression (18–21) Zekioglu et al.(18) reported the percentages of ER and PR positivity to be 68% and 61% and the prevalence of c-erbB-2 and p53 proteins to be 54% and 48%, respectively, for IMPCs. Walsh and Bleiweiss (20) reported high percentages of ER and PR positivity (90% and 70%, respectively) and nearly double the expected percentage of c-erbB-2 positivity (60%). These results are higher than those of common breast cancers including IDCs. Yun et al.(21) reported high percentages of ER and lower percentage of PR positivity (93% and 52%, respectively). In our study, the expressions of ER (81%) and PR (71%) were higher than the results of the previous studies. The prevalence of c-erbB-2 (43%) was lower than the result of previous studies for IMPCs, but higher than the prevalence of common breast cancers.

The percentage of hormone receptor positivity for IMPC is higher than for invasive ductal carcinoma, but ER and PR positivity or expression of c-erbB-2 or p53 are not reliable criteria for the discrimination of IMPC from conventional invasive ductal carcinoma (18). High expression of c-erbB-2 and p53, high proliferation index, low expression of steroid hormone receptors are related to the unfavorable prognostic factors (17).

Our study had some limitations. First, this is a single-institution data set and the patients were retrospectively analyzed and thus the possibility of selection bias should be considered. The category and image findings of tumors could be overestimated because of the reviewers knew the pathologic result of the tumors. However, we attempted to recruit consecutive patients in order to avoid any selection bias. Second, the study lacks a control group composed of patients who were diagnosed with IDC, not otherwise specified (IDC, NOS). Third, we could not analyze new imaging modality, such as elastography on sonography and diffusion weighted image (DWI) or spectroscopy on MR imging, which can aid in differentiation of subtype of breast cancer. Further study using elastography,

DWI and spectroscopy in patients with IPMC would be necessary to better understand the difference between IDC and IPMC.

In conclusion, dynamic MR imaging may be used for better delineation of disease extent in IMPC of the breast than can be obtained with sonography or mammography, and it has a role in surgical planning. IMPC manifested as typical malignant morphologic features with washout pattern on MR imaging, and multiplicity and combined pattern were common.

Axillary lymph node metastasis is commonly associated and this is the hallmark of IMPC. Awareness of these MR imaging findings should be helpful to predict IMPC and to decide aggressive surgical plan including axillary surgery.

## References


1. Siriaunkgul, S. and F.A. Tavassoli, Invasive micropapillary carcinoma of the breast. Mod Pathol 1993;6:660-662
2. Petersen, JL. Breast carcinomas with an unexpected inside-out growth pattern: rotation of polarization associated with angioinvasion (abstr). Pathol Res Pract 1993;189:780-784
3. Luna-Moré S, Gonzalez B, Acedo C, Rodrigo I, Luna C. Invasive micropapillary carcinoma of the breast. A new special type of invasive mammary carcinoma. Pathol Res Pract 1994;190:668-674
4. Middleton LP, Tressera F, Sobel ME, et al. Infiltrating micropapillary carcinoma of the breast. Mod Pathol 1999;12:499-504
5. Nassar H, Wallis T, Andea A, Dey J, Adsay V, Visscher D. Clinicopathologic analysis of invasive micropapillary differentiation in breast carcinoma. Mod Pathol 2001;14:836-841
6. Paterakos M, Watkin WG, Edgerton SM, Moore DH 2nd, Thor AD. Invasive micropapillary carcinoma of the breast: a prognostic study. Hum Pathol 1999;30:1459-1463
7. Adrada B, Arribas E, Gilcrease M, Yang WT. Invasive micropapillary carcinoma of the breast: mammographic, sonographic, and MRI features. AJR Am J Roentgenol 2009; 193:W58-63
8. Günhan-Bilgen I, Zekioglu O, Ustün EE, Memis A, Erhan Y. Invasive micropapillary carcinoma of the breast: clinical, mammographic, and sonographic findings with histopathologic correlation. AJR Am J Roentgenol 2002;179:927-931
9. Radiology, A.C.o., Mammography, in Breast imaging reporting and data system (BI-RADS). 2003, American College of Radiology: Reston
10. Soo MS, Williford ME, Walsh R, Bentley RC, Kornguth PJ. Papillary carcinoma of the breast: imaging findings. AJR Am J Roentgenol 1995;164:321-326
11. Muttarak M, Lerttumnongtum P, Chaiwun B, Peh WC. Spectrum of papillary lesions of the breast: clinical, imaging, and pathologic correlation. AJR Am J Roentgenol 2008;191:700-707
12. Ibarra JA. Papillary lesions of the breast. Breast J 2006;12: 237-251
13. Kim DS, Nariya C, Ko ES, et al. Imaging and the clinical-pathologic features of invasive micropapillary carcinoma of the breast. J Korean Radiol Soc 2007;56:497-503
14. Chiou HJ, Chou YH, Chiou SY, et al. Superficial soft-tissue lymphoma: sonographic appearance and early survival. Ultrasound Med Biol 2006;32:1287-1297
15. Daniel BL, Yen YF, Glover GH, et al. Breast disease: dynamic spiral MR imaging. Radiology 1998;209:499-509
16. Snow RD, Dyess DL, Harpen MD, Kreisberg CN, Tucker JA. Dynamic magnetic resonance imaging in evaluating suspicious breast lesions: correlation with pathologic findings. South Med J 1998;91:527-532
17. Pettinato G, Manivel CJ, Panico L, Sparano L, Petrella G. Invasive micropapillary carcinoma of the breast: clinicopathologic study of 62 cases of a poorly recognized variant with highly aggressive behavior. Am J Clin Pathol 2004;121:857-866
18. Zekioglu O, Erhan Y, Ciris M, Bayramoglu H, Ozdemir N. Invasive micropapillary carcinoma of the breast: high incidence of lymph node metastasis with extranodal extension and its immunohistochemical profile compared with invasive ductal carcinoma. Histopathology 2004;44:18-23
19. Luna-Moŕe S, de los Santos F, Bretón JJ, Cañadas MA. Estrogen and progesterone receptors, c-erbB-2, p53, and Bcl-2 in thirty-three invasive micropapillary breast carcinomas. Pathol Res Pract 1996;192:27-32
20. Walsh, M.M. and I.J. Bleiweiss, Invasive micropapillary carcinoma of the breast: eighty cases of an underrecognized entity. Hum Pathol 2001;32:583-589
21. Yun SU, Choi BB, Shu KS, et al. Imaging findings of invasive micropapillary carcinoma of the breast. J Breast Cancer 2012; 15:57-64

대한자기공명의과학회지 16:205-216(2012)

# 유방의 침윤성 미세유두상암: 유방촬영, 초음파와 자기공명영상 소견

성균관대학교 의과대학 삼성서울병원 영상의학과

**이선정 · 한부경 · 고은영 · 신정희**

**목적**: 유방의 침윤성 미세유두상암의 특징적인 영상소견과 임상병리학적 특징에 대해 알아보고자 하였다.

**대상과 방법**: 본원에서 2005년부터 2009년까지 4년간 미세유두상암으로 수술 받은 47명의 환자들 중, 수술 전 유방촬영, 초음파, 자기공명영상을 시행한 32명의 환자를 대상으로 하였다. 두 명의 영상의학과 의사가 후향적으로 영상소견과, 임상증상, 조직학적 결과를 분석하였다.

**결과**: 유방촬영에서 32명중 29명의 환자가 유방암 의심소견을 보였으며, 석회화를 동반한 종괴 또는 비대칭이 가장 흔한(15/32, 65%) 소견이었다. 석회화는 20명(63%)의 환자에서 나타났으며, 석회화의 모양은 주로 무정형 또는 점상형이었다(n = 12, 60%). 유방초음파와 자기공명영상에서 모든 병변은 유방암 의심소견이었다. 가장 흔한 초음파 소견은 단발성(n = 20) 또는 다발성(n = 10) 의 불규칙한 저에코의 종괴였으며, 종괴들은 주로 저에코로 보였다(n = 29, 97%). 자기공명영상에서, 병변은 단발성 또는 다발성의 종괴가 23명(72%)에서 보였으며, 6명에서는 종괴와 비종괴 조영증강이 함께 있었고, 3명에서 비종괴 조영증강 병변으로 보였다. 조직학적으로 액와림프절 전이는 흔한 소견이었다(25/32, 78%). 임상증상이 없는 경우는 드물었다(9/32, 28%).

**결론**: 유방의 침윤성 미세유두상암의 특징적인 영상소견은 악성종양을 시사한다. 유방촬영에서 미세석회화, 유방초음파에서 저에코성 병변, 자기공명영상에서 때로는 비종괴 조영증강을 동반한 불규칙한 종괴가 흔한 소견이었다. 액와림프절 전이도 흔히 동반되는 소견이었다.

통신저자 : 한부경, (135-710) 서울시 강남구 일원동 50, 성균관대학교 의과대학 삼성서울병원 영상의학과
Tel. (02) 3410-0517 Fax. (02) 3410-0084 E-mail: bkhan@skku.edu